Commun. Theor. Phys. **67** (2017) 443–448 Vol. 67, No. 4, April 1, 2017

Numerical Investigation of Micropolar Casson Fluid over a Stretching Sheet with Internal Heating

Zaffar Mehmood,* R. Mehmood, and Z. Iqbal

Department of Mathematics, HITEC University, Taxila, Pakistan

(Received September 29, 2016; revised manuscript received December 12, 2016)

Abstract *This theoretical study investigates the microrotation effects on mixed convection flow induced by a stretching sheet. Casson fluid model along with microrotation is considered to model the governing flow problem. The system is assumed to undergo internal heating phenomenon. The governing physical problem is transformed into system of nonlinear ordinary differential equations using scaling group of transformations. These equations are solved numerically using Runge Kutta Fehlberg scheme coupled with shooting technique. Influence of sundry parameters for the case of strong and weak concentration of microelements on velocity, temperature, skin friction and local heat flux at the surface are computed and discussed. Lower skin friction and heat flux is observed for the case of weak concentration ($n = 0.5$) compared to strong concentration of microelements ($n = 0.0$) near the wall.*

PACS numbers: 44.25.+f, 47.10.ad, 47.50.-d **DOI:** 10.1088/0253-6102/67/4/443
Key words: micropolar, Casson fluid, mixed convection, internal heating, numerical solution

1 Introduction

Fluids with microstructures are termed as micropolar fluids. These fluids comprise of rigid, randomly oriented particles submerged in a glutinous medium. Micropolar fluids find tremendous applications in blood, foodstuffs, polymers, liquid metal and alloys, plasma and drilling of oil and gas wells etc. Such type of fluid model contains non-symmetric stress tensors. Eringen[1−2] introduced the theoretical explanations of micropolar fluids and discovered the effects of micro motion of fluid elements. He proposed a logical and significant overview of the classical Navier–Stokes model, covering, both in theory and applications, many more phenomena than the classical one. Moreover his generalization was well-designed and not too complex. Airman *et al.*[3−4] presented a detailed review on application of fluids experiencing micro rotation at particle level. Khonsari and Brewe[5] examined the effects of viscous dissipation on lubrication characteristics of micropolar fluids. They reported that existence of microstructure, according to the micropolar theory, tends to enhance the load-carrying capacity and friction coefficient. Rotating micropolar fluid between parallel plates with heat transfer under the influence of transverse magnetic field has been investigated by Rashid *et al.*[6] They concluded that the micro rotation is an increasing function of coupling parameter, magnetic field and Reynolds number for strong concentration and it is a decreasing function of viscosity parameter. Nazar *et al.*[7] analyzed the stagnation point flow of a micropolar fluid over a stretching sheet. They carried out numerical investigation by employing Keller Box method. Non-Newtonian fluids have been an intense topic of research for the past few decades. Much focus had been given to the modeling and analysis of non-Newtonian fluids with rheological characteristics because of usage of various non-Newtonian fluids such as lubricants in industry. The non-linearity can manifest itself in a variety of ways in many fields, such as in food processing, drilling operations and bio-engineering. In this regard Ellahi *et al.*[8] presented numerical analysis of MHD steady non-Newtonian flows in presence of heat transfer and nonlinear slip effects. Similarly, Makinde *et al.*[9] analyzed unsteady flow of a reactive variable viscosity non-Newtonian fluid through a porous saturated medium with asymmetric convective boundary conditions and observe that there is a transient increase in both fluid velocity and temperature with an increase in the reaction strength, viscous heating and fluid viscosity parameter. Among the class of several other non-Newtonian fluid models, Casson fluid is one such model with yield stress characteristics. Casson fluid falls in the category of dilatant fluids. It is assumed that Casson fluid has an infinite viscosity at zero shear rates. If the applied shear stress is less than the yield stress then fluid behave like a solid and when shear stress applied is greater than yield stress fluid starts to move. Casson fluid model best fit to rheological data for numerous materials such as jelly, sauce, honey, soup and concentrated fruit juices, etc.[10] The presence of protein, fibrinogen and globulin in aqueous base plasma, red blood cells makes human blood an ideal example of Casson fluid. Number of researchers used Casson fluid to mathemati-

*Corresponding author, E-mail: zaffarilyas@gmail.com

cally model and examine the blood flow under a low shear rate in narrow arteries. Shahzad *et al.*[11] studied effects of mass transfer on generalized non-Newtonian fluid. They analyzed the influence of chemical reaction and suction on Casson fluid in presence of magnetic field. Nadeem *et al.*[12] observed analytically flow of Casson nanofluid. Mustafa *et al.*[13] discussed unsteady boundary layer flow of a Casson fluid due to an impulsively started moving flat plate. Similarly Bhattacharya *et al.*[14] presented analytic solution for magneto hydrodynamic boundary layer flow of Casson fluid over a stretching/shrinking sheet with wall mass transfer. Heat transfer of viscous non-Newtonian fluids past a stretching sheet is a considerable problem in fluid dynamics. The problems arise in the field of engineering and metallurgy depends on hydrodynamic flow and heat transfer rate. In polymer technology, stretching plastic sheets are used in manufacturing products. In electrically conducting fluids, strips are used to control the cooling process. Chen[15] worked out laminar mixed convection of stretching sheet adjacent to vertical wall. Ali *et al.*[16] examined laminar mixed convection boundary layers induced by a linearly stretching permeable surface. Ishak *et al.*[17] inspected mixed convection boundary layers in the stagnation-point flow toward a stretching vertical sheet. The thermal effects in fluid flows may cause heat transfer effects in manufacturing processes. In these processes, thermal buoyancy force arises due to heating of a surface that may be in rest or moving continuously under some circumstances. Shateyi *et al.*[18] analyzed the effects of thermal radiation, hall currents, soret and dufour on MHD flow and heat and mass transfer in a micro polar fluid by mixed convection over stretching surfaces in porous media. Vajravelu *et al.*[19] studied the heat transfer in a viscous fluid over a stretching sheet with viscous dissipation and internal heat generation. Some more studies related to the current topic can be found in Refs. [20–31].

Most of researches have been carried out in micro polar fluids for characterizing the impact of magnetic field, heat transfer, mixed convection and viscous dissipation etc. To the best of our knowledge, micro polar fluids with rheological characteristics have not been discussed in past. Novelty of present study is to examine micro polar Casson fluid towards a stretching sheet influenced by internal heat generation. Recent research is a fresh contribution in this regard. Effects of sundry parameters on flow and heat transfer characteristics are examined and discussed in a physical manner.

2 Mathematical Formulation

Consider steady 2D flow of an incompressible micropolar Casson fluid towards a linear stretching convective sheet. Heat and mass transfer flow due to stretching of a heated or cooled surface of variable temperature $T(x)$ and uniform ambient temperature is T_∞ ($T > T_\infty$) is considered. The governing equations of motion (i.e. the continuity, momentum, energy) in vector form for micropolar fluid with rheological characteristics are as follow:

$$\nabla \cdot \bar{V} = 0\,, \tag{1}$$

$$\rho(\bar{V}\cdot\nabla)\bar{V} = k(\nabla\times N) + m(T-T_\infty)\bar{g} + \mu\Big(1+\frac{1}{\beta}+k\Big)(\nabla^2\bar{V})\,, \tag{2}$$

$$\rho j(\bar{V}\cdot\nabla)\bar{N} = k(\nabla\times\bar{V}) - 2k\bar{N} - \gamma(\nabla^2\bar{N})\,, \tag{3}$$

$$\bar{V}\cdot\nabla T = \alpha\nabla^2 T + \frac{Q_0}{\rho C_p}(T-T_\infty)\,. \tag{4}$$

Component form of Eqs. (1)–(4) under boundary layer approximations and considering buoyancy effects are given by:

$$\frac{\partial u}{\partial x} + \frac{\partial v}{\partial y} = 0\,, \tag{5}$$

$$u\frac{\partial u}{\partial x} + v\frac{\partial u}{\partial y} = \nu\Big(1+\frac{1}{\beta}\Big)\Big(\frac{\partial^2 u}{\partial y^2}\Big) + \frac{g_0 m(T-T_\infty)}{\rho} + \frac{k}{\rho}\frac{\partial^2 u}{\partial x^2} + \frac{k}{\rho}\frac{\partial N}{\partial y}\,, \tag{6}$$

$$u\frac{\partial N}{\partial x} + v\frac{\partial N}{\partial y} = \frac{\gamma}{\rho j}\frac{\partial^2 N}{\partial y^2} - \frac{\gamma}{\rho j}\Big(2N + \frac{\partial u}{\partial y}\Big)\,, \tag{7}$$

$$u\frac{\partial T}{\partial x} + v\frac{\partial T}{\partial y} = \frac{\kappa}{\rho C_p}\frac{\partial^2 T}{\partial y^2} + \frac{Q_0}{\rho C_p}(T-T_\infty)\,, \tag{8}$$

with appropriate boundary conditions

$$u = u_w(x) = ax, \quad v = 0, \quad N = -n\frac{\partial u}{\partial y}\,,$$

$$-k\frac{\partial T}{\partial y} = h_f(T_f - T), \quad \text{as} \quad y = 0\,, \tag{9}$$

$$u \to 0, \quad N \to 0, \quad T \to T_\infty, \quad \text{as} \quad y \to \infty\,, \tag{10}$$

where in above equations u and v are velocity components along coordinates axes, $u_w(x)$ is velocity at wall, $a > 0$ is stretching parameter, ρ is fluid density, ν is kinematic viscosity, k is vortex viscosity, β ($= \mu_B\sqrt{2\pi_c}/p_y$) is Casson fluid parameter, N is micropolar rotation velocity, n is boundary concentration parameter of fluid, the case $n = 0$ represents strong concentration, $n = 0.5$ indicates weak concentration, C_p is the specific heat at constant pressure p, κ is thermal conductivity of the medium and T is fluid temperature. A stream of cold fluid at temperature T_∞ is moving over sheet while the surface of sheet is heated from below by convection from hot fluid at temperature T_f which provides a heat transfer coefficient h_f, g_0 is acceleration due to gravity, m is coefficient of thermal expansion, Q_0 is heat generation coefficient, γ is spin radiation viscosity defined as $\gamma = (\mu + k/2)j$ where $j = \nu/a$ is the micro-inertia density.

To convert above system of partial differential equations, we introduce following similarity transformations[32]

$$\eta = \sqrt{\frac{a}{\nu}}y, \quad u = axf'(\eta), \quad v = -\sqrt{a\nu}f(\eta)\,,$$

$$N = a\sqrt{\frac{a}{\nu}}xg(\eta), \quad \text{and} \quad \theta(\eta) = \frac{T - T_\infty}{T_w - T_\infty}. \tag{11}$$

Equation (5) is automatically satisfied and Eqs. (6)–(8) become

$$\Big(1 + \frac{1}{\beta} + K\Big)f''' + ff'' - (f')^2 + \lambda\theta + Kg' = 0, \tag{12}$$

$$\Big(1 + \frac{K}{2}\Big)g'' - fg' + gf' - K(2g + f'') = 0, \tag{13}$$

$$\theta'' + \Pr f\theta' + \Pr \delta\theta = 0, \tag{14}$$

and corresponding boundary conditions in Eqs. (9) and (10) take the form

$$\begin{aligned} &f(\eta) = 0, \quad f'(\eta) = 1, \quad g(\eta) = -nf''(\eta), \\ &\theta'(\eta) + Bi(1 - \theta(\eta)) = 0, \quad \text{as} \quad \eta = 0, \\ &f'(\eta) \to 0, \quad g(\eta) \to 0, \quad \theta(\eta) \to 0, \quad \text{as} \quad \eta \to \infty, \end{aligned} \tag{15}$$

where K is micropolar parameter, λ is thermal convective parameter, Pr is the Prandtl number, δ is heat generation parameter and Bi is Biot number which are defined as:

$$\begin{aligned} &Pr = \frac{\mu c_p}{\kappa}, \quad K = \frac{k}{\mu}, \quad \lambda = \frac{G_r}{Re_x^2}, \\ &\delta = \frac{Q_0}{a\rho C_p}, \quad Bi = \frac{h_f}{k}\sqrt{\frac{\nu}{a}}, \end{aligned} \tag{16}$$

where G_r is Grashof number and Re_x is Reynold number are given by the relations

$$G_r = \frac{g_0\beta(T - T_\infty)}{\nu^2}, \quad Re_x^2 = \frac{xu_0(x)}{\nu}. \tag{17}$$

The physical quantities of interest are skin friction coefficient C_f and local Nusselt number Nu_x which are defined as

$$C_f = \frac{\tau_w}{\rho u_w^2}, \quad Nu_x = \frac{xq_w}{k(T_w - T_\infty)}, \tag{18}$$

where the wall friction τ_w and heat transfer at wall q_w, are expressed as

$$\begin{aligned} &\tau_w = \Big(\mu + \frac{p_y}{\sqrt{2\pi_c}} + k\Big)\frac{\partial u}{\partial y} + kN|_{y=0}, \\ &q_w = -\kappa\Big(\frac{\partial u}{\partial y}\Big) \quad \text{at} \quad y = 0. \end{aligned} \tag{19}$$

In view of Eq. (19), expressions described in (18) provide the skin friction and local Nusselt number as

$$\begin{aligned} &C_f Re_x^{1/2} = \Big(1 + \Big(\frac{1}{\beta}\Big) + K(1 - n)\Big)f''(0), \\ &Nu_x Re_x^{-1/2} = -\theta'(0), \end{aligned} \tag{20}$$

in which $Re_x = ax/\nu$ is local Reynolds number.

3 The Numerical Solutions

Shooting method along with Runge Kutta fifth order technique was incorporated to tackle the system of nonlinear differential equations. Thus, solution of coupled nonlinear governing boundary layer Eqs. (12)–(14) together with boundary conditions in Eq. (15) are computed by means of shooting method along Runge Kutta fifth order technique. Initially higher order nonlinear differential equations (12)–(14) are converted into a system of first order differential equations and further transformed into initial value problem by labeling the variables as

$$\begin{pmatrix} y_1' \\ y_2' \\ y_3' \\ y_4' \\ y_5' \\ y_6' \\ y_7' \end{pmatrix} = \begin{pmatrix} y_2 \\ y_3 \\ \frac{1}{(1+\frac{1}{\beta}+K)}(-y_1y_3 + (y_2)^2 - \lambda y_6 - Ky_5) \\ y_5 \\ \frac{1}{(1+\frac{K}{2})}(y_1y_5 - y_4y_2 + K(2y_4 + y_3)) \\ y_7 \\ -Pry_1y_7 - Pr\delta y_6 \end{pmatrix}. \tag{21}$$

Associated boundary conditions in Eq. (15) can be transformed as

$$\begin{pmatrix} y_1(0) \\ y_2(0) \\ y_3(0) \\ y_4(0) \\ y_5(0) \\ y_6(0) \\ y_7(0) \end{pmatrix} = \begin{pmatrix} 0 \\ 1 \\ S_1 \\ -nS_1 \\ S_2 \\ S_3 \\ -Bi(1 - S_3) \end{pmatrix}. \tag{22}$$

Above nonlinear coupled ODEs along with initial conditions are solved using Runge Kutta method of order 5 integration techique. Appropriate values of unknown initial conditions S_1, S_2 and S_3 are approximated through Newton's method. Computations are carried out using mathematics software *MATLAB*. End of boundary layer region i.e., when $\eta \to \infty$ to each group of parameters, is determined when the values of unknown boundary conditions at $y = 1$ do not change to a successful loop with error less than 10^{-6} (see Refs. [33–34]).

4 Results and Discussion

This section is dedicated to examine the influence of sundry parameters on velocity $f'(\eta)$, microrotation $g(\eta)$ and temperature profile $\theta(\eta)$ in the presence of strong ($n = 0$) and weak ($n = 0.5$) concentrations. Figure 1 is plotted to discover influence of micropolar parameter K on velocity profile $f'(\eta)$ for the case of weak concentration. It can be observed that velocity profile $f'(\eta)$ as well as corresponding momentum boundary layer thickness rises with the increasing behavior of micropolar parameter K for weak concentration. Figure 2 depicts that microrotation profile $g(\eta)$ increases with micropolar parameter K near the wall for both cases of concentration but reverse behavior is observed away from surface. Figure 3 depicts the influence of mixed convection parameter λ on microrotation profile $g(\eta)$ for strong as well as weak concentrations is positive. Influence of Casson fluid parameter β on microrotation profile $g(\eta)$ is presented through Fig. 4. It is quite evident that microrotation profile $g(\eta)$ is higher for the case of weak concentration ($n = 0.5$) as compared to strong concentration ($n = 0$). The graph for various

values of Biot number Bi for temperature profile $\theta(\eta)$ is displayed in Fig. 5. It can be seen that temperature increases with attractive conduct of Biot number Bi. Figure 6 is plotted to examine the effect of δ on temperature profile $\theta(\eta)$ for weak concentration $n = 0.5$. Here a grow in temperature and thermal boundary layer thickness is observed for mount in δ for weak concentration $n = 0.5$.

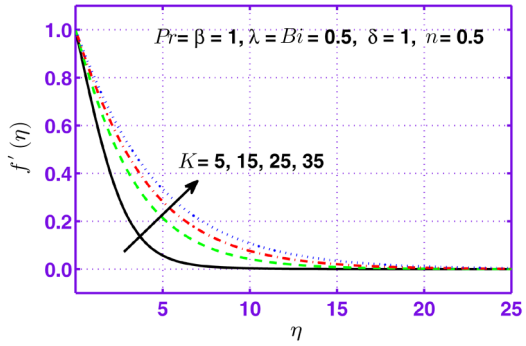

Fig. 1 Behavior of velocity profile $f'(\eta)$ against K.

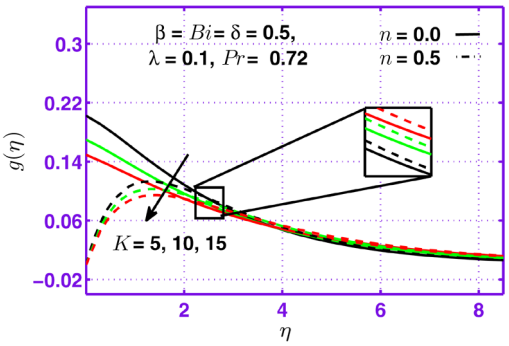

Fig. 2 Behavior of microrotation profile $g(\eta)$ against K.

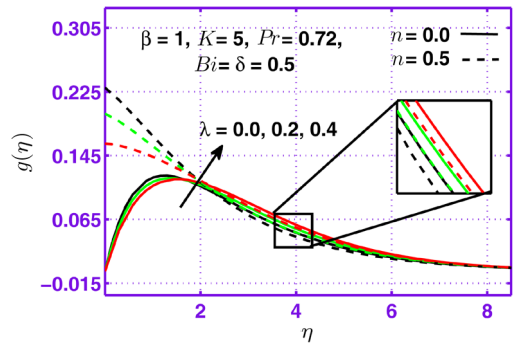

Fig. 3 Behavior of microrotation profile $g(\eta)$ against λ.

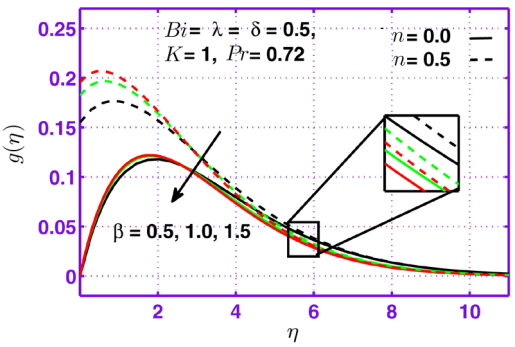

Fig. 4 Behavior of microrotaion profile aganist β for $n = 0$ and $n = 0.5$.

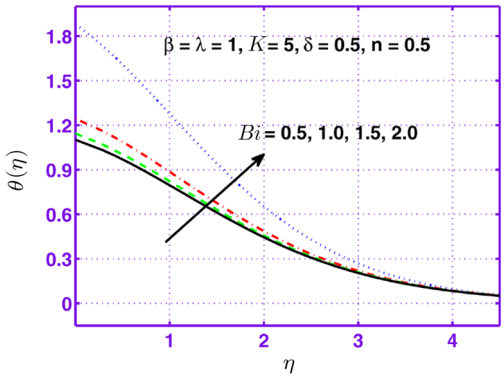

Fig. 5 Behavior of temperature profile $\theta(\eta)$ against Biot number Bi.

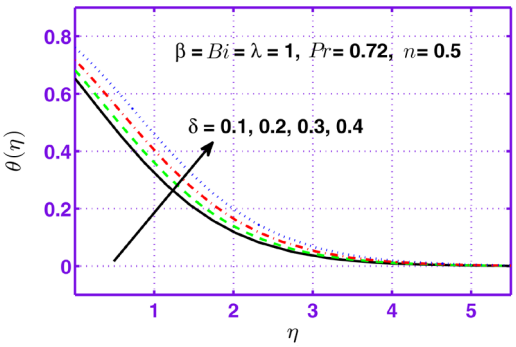

Fig. 6 Behavior of temperature profile $\theta(\eta)$ against δ.

To investigate effects of parameters on skin friction coefficient $(-f''(0))$ and local Nusselt number $(-\theta'(0))$ we have demonstrated Figs. 7–10. From Fig. 7 it is illustrated that skin friction lessens by rising fluid parameter β for strong as well as weak concentrations. The behavior of micropolar parameter K on skin friction is seen in Fig. 8. It explains that skin friction is a decreasing function of β as micropolar parameter K increases. Moreover, Fig. 9 demonstrates the effect of micropolar parameter K on Nusselt number $(-\theta'(0))$ when plotted against fluid parameter β. Heat flux $(-\theta'(0))$ for weak $(n = 0.5)$ and strong $(n = 0.0)$ concentrations is displayed in Fig. 10. It is observed that heat flux $(-\theta'(0))$ as a function of micropolar parameter K falls with growing values of fluid parameter β. Effects for concerning parameters have similar behavior as in skin friction for both cases of concentration.

5 Concluding Remarks

The aim of this study is to investigate microrotation effects on mixed convective flow of a Casson fluid induced

by a stretching sheet. The governing physical problem is tackled numerically using Runge Kutta Fehlberg scheme coupled with shooting. The core outcomes of this study are:

- The velocity profile $f'(\eta)$ and microrotation profile $g(\eta)$ depict opposite behavior against micropolar parameter K.
- Microrotation profile $g(\eta)$ rises with mixed convective parameter λ while it decreases with Casson fluid parameter β for strong as well as weak concentration.
- Skin friction coefficient $-f''(0)$ and local Nusselt number $-\theta'(0)$ rise with micropolar parameter K while decrease with Casson fluid parameter β.
- Higher skin friction coefficient $-f''(0)$ and local Nusselt number $-\theta'(0)$ are observed for the case of strong concentration ($n = 0$) compared to weak concentration ($n = 0.5$).

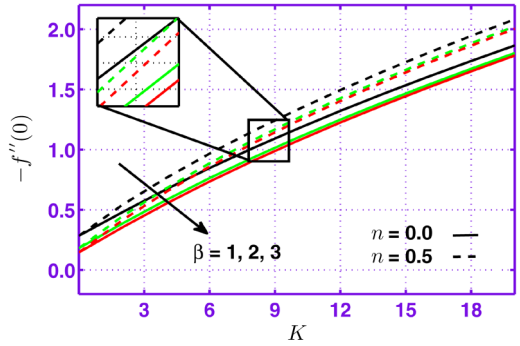

Fig. 7 Behavior of skin friction coefficient aganist K for different values of β.

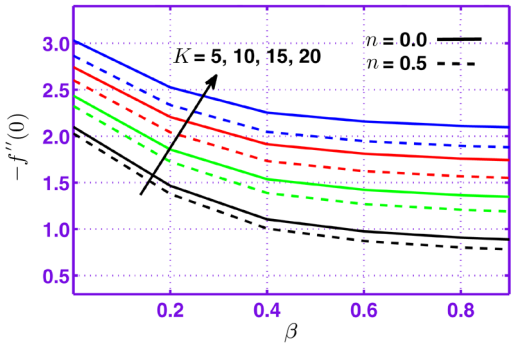

Fig. 8 Behavior of skin friction coefficient aganist β for different values of K.

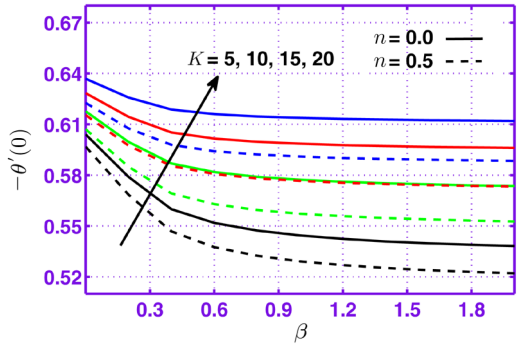

Fig. 9 Behavior of Nusselt number aganist K for different values of β.

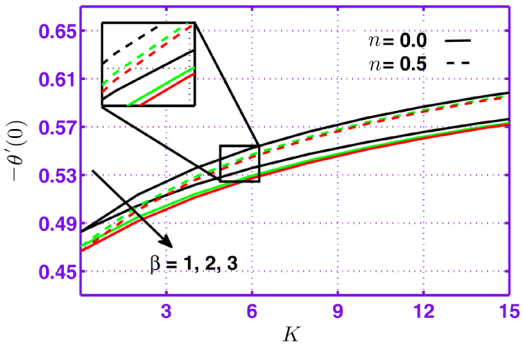

Fig. 10 Behavior of skin friction coefficient aganist β for different values of K.

References

[1] A. C. Eringen, Int. J. Engg. Sci. **2** (1964) 205.

[2] A. C. Eringen, J. Math. Mech. **16** (1966) 1.

[3] T. Ariman, M. A. Turk, and N. D. Sylvester, Int. J. Engg. Sci. **11** (1973) 905.

[4] T. Ariman, M. A. Turk, and N. D. Sylvester, Int. J. Engg. Sci. **12** (1974) 273.

[5] M. M. Khonsari and D. E. Brewe, Acta Mech. **105** (1994) 57.

[6] R. Mehmood, S. Nadeem, and S. Masood, J. Magn. Magn. Mat. **401** (2016) 1006.

[7] R. Nazar, N. Amin, D. Filip, and I. Pop, Int. J. Nonlinear Mech. **39** (2004) 1227.

[8] R. Ellahi and M. Hameed, Int. J. Num. Meth. Heat Fluid Flow **22** (2012) 24.

[9] O. D. Makinde, T. Chinyoka, and L. Rundora, Comp. Math. Appl. **62** (2011) 3343.

[10] N. Casson, *Rheology of Disperse Systems in Flow Equation for Pigment Oil Suspensions of the Printing Ink Type*, *Rheology of disperse systems*, C. C. Mill, Ed., 84–102, Pergamon Press, London, U. K. (1959).

[11] S. A. Shahzad, T. Hayat, M. Qasim, and S. Asghar, J. Chem. Engg. **30** (2013) 187.

[12] S. Nadeem, R. Mehmood, and N. S. Akbar, Int. J. Thermal Sci. **78** (2014) 90.

[13] M. Mustafa, T. Hayat, I. Pop, and A. Aziz, Heat Transf. – Asian Res. **40** (2011) 563.

[14] K. Bhattacharyya, T. Hayat, and A. Alsaedi, Chin. Phys. B **22** (2013) 024702.

[15] C. H. Chen, J. Heat Mass Transf. **33** (1998) 471.

[16] M. E. Ali and F. Al-Yousef, Int. J. Heat Mass Transf. **45** (2002) 4241.

[17] A. Ishak, R. Nazar, and I. Pop, Meccanica **41** (2006) 509.

[18] S. Shateyi, S. S. Motsa, and P. Sibanda, Math. Prob. Eng. **2010** (2010) 1.

[19] K. Vajravelu and A. Hadjinicolaou, Int. Commun. Heat Mass Transfer **20** (1993) 417.

[20] C. H. Chen, Int. J. Non-Linear Mech. **44** (2009) 596.

[21] M. M. Rashidi and S. Abbasbandy, Commun. Nonlin. Sci. Num. Simul. **16** (2011) 1874.

[22] N. T. M. Eldabe and M. G. E. Salwa, J. Phys. Soc. Jpn. **64** (1995) 41.

[23] S. Nadeem, R. Mehmood, and N. S. Akbar, J. Comput. Theor. Nano Sci. **11** (2014) 1422.

[24] I. Pop and D. B. Ingham, *Convective heat transfer. Mathematical and computational modeling of viscous fluids and porous media pergamon*, Oxford, (2001).

[25] O. D. Makinde, Int. J. Phys. Sci. **5** (2010) 700.

[26] A. Ishak, Appl. Math. Comput. **217** (2010) 837.

[27] O. D. Makinde and P. O. Olanrewaju, Trans. ASME J. Fluid Eng. **132** (2010) 044502.

[28] M. M. Nandeppanavar, K. Vajravelu, M. Subhas Abel, and M. N. Siddalingappa, Meccanica **48** (2013) 1451.

[29] T. F. Lin, C. J. Chang, and W. M. Yan, J. Heat Transf. **110** (1988) 337.

[30] M. V. Karwe and Y. Jaluria, Int. J. Heat Mass Transfer **35** (1992) 493.

[31] N. A. Yacob, A. Ishak, I. Pop, and K. Vajravelu, Nanoscale Research Lett. **6** (2011) 1.

[32] M. Qasim, I. Khan, and S. Shafie, Plos ONE **8** (2013) 49045.

[33] Z. Mehmood and Z. Iqbal, J. Mol. Liq. **224** (2016) 1083.

[34] E. Azhar, Z. Iqbal, and E. N. Maraj, Zeitschrift fr Naturforschung A **71** (2016) 837848.